Probing the Active Site Steric Flexibility of HIV-1 Reverse Transcriptase: Different Constraints for DNA- versus RNA-Templated Synthesis[†]

Adam P. Silverman,[‡] Scott J. Garforth,[§] Vinayaka R. Prasad,[§] and Eric T. Kool*[,‡]

Department of Chemistry, Stanford University, Stanford, California 94305-5080, and Department of Microbiology and Immunology, Albert Einstein College of Medicine, Bronx, New York 10461

Received December 12, 2007; Revised Manuscript Received February 18, 2008

ABSTRACT: The steric flexibility or rigidity of polymerase active sites may play an important role in their fidelity of nucleic acid synthesis. In this regard, reverse transcriptases offer an unusual opportunity to compare two enzymatic activities that proceed in the same active site. For HIV-1 reverse transcriptase, reverse transcription (RNA-templated synthesis) is known to proceed with lower fidelity than DNA-templated synthesis. Here, we describe the use of a set of variably sized nonpolar thymidine and uracil mimics as molecular rulers to probe the active site steric constraints of HIV-1 RT, and for the first time, we directly compare the functional flexibility of these two activities. Steady-state kinetics of incorporation for natural dNTPs opposite unnatural template bases as well as for unnatural dNTPs opposite natural template bases are reported for the DNA-templated DNA synthesis, and comparison is made with recent data for the RNA-templated activity. Kinetics for extension beyond a base pair containing the analogue template bases are also reported both for RNA and DNA templates. Our results show that the DNA-dependent polymerization by HIV-RT is highly sensitive to size, strongly biasing against both too-small and too-large base pairs, while, by contrast, the RNA-dependent polymerization is only biased against analogues that are too small, and is much more accepting of larger base pairs. In addition, base pair extension with HIV-RT is found to be relatively insensitive to varied base pair size, consistent with its high mutagenicity. Overall, the data show greater rigidity with a DNA template as compared with an RNA template, which correlates directly with the higher fidelity of the DNA-templated synthesis. Possible structural explanations for these differences are discussed. We also report kinetics data for two HIV-1 RT mutants reported to have altered fidelity (F61A and K65R) using DNA templates containing nonpolar base analogues, and find that one of these (F61A) is a high-fidelity enzyme that appears to be sensitive to a loss of hydrogen-bonding groups.

The reverse transcriptase of the HIV-1[1] virus (HIV-RT) is responsible for the replication of the RNA genome of the infectious agent and has been widely studied because of its importance as a drug target in the treatment of human retroviral infection (*1–4*). The enzyme serves both to synthesize a DNA complement of the RNA genome and also to synthesize a second cDNA strand from this first DNA copy. The degree of accuracy by which these copies are made is medically important since errors allow the virus to mutate, resulting in drug resistance. Significantly, the enzyme is known to synthesize DNA with lower fidelity when it is copying an RNA template than with a DNA template (*5, 6*); however, the physical origins of this difference are not known.

The efficiency and fidelity of DNA replication enzymes are determined by a number of factors, and steric effects in the polymerase active site are believed to be among the most important contributors (*7–10*). To measure such steric factors in a functional way, we recently developed a series of nonpolar thymidine analogues of systematically varied size (*11*). These C-nucleoside analogues retain the shape of natural thymidine but are unable to form canonical Watson–Crick hydrogen bonds. The carbonyl oxygens are replaced with either hydrogen or halogens to make the analogues dH, dF, dL, dB, and dI; these vary in size by only 1.0 Å across the entire series (Figure 1). The difluorotoluene analogue dF is nearly identical in size and shape to natural thymidine (*12, 13*), while the toluene analogue dH is smaller, and the dichloro-, dibromo-, and diiodo-toluene analogues are increasingly larger. These analogues were previously used to probe active site steric effects with the Klenow fragment of *E. coli* DNA Pol I (Kf exo$^-$), and it was discovered that both the efficiency and fidelity of the enzyme were highly sensitive to the subangstrom size differences across the series (*14*). The nonpolar bases were preferentially paired with adenine, consistent with their thymine-mimicking shape, and at the optimum size, showed efficiency and selectivity close

[†] This work was supported by the U.S. National Institutes of Health (GM072705). A.S. acknowledges support from an NSF Graduate Fellowship and a Lieberman Fellowship.

* To whom correspondence should be addressed. Eric T. Kool, Department of Chemistry, Stanford University, Stanford, CA 94305. Phone: (650) 724-4741. Fax (650) 725-0259. E-mail: kool@stanford.edu.

[‡] Stanford University.

[§] Albert Einstein College of Medicine.

[1] HIV-1, human immunodeficiency virus 1; RT, reverse transcriptase; DDDP, DNA template-dependent DNA polymerization; RDDP, RNA template-dependent DNA polymerization.

10.1021/bi702427y CCC: $40.75
Published on Web 03/27/2008

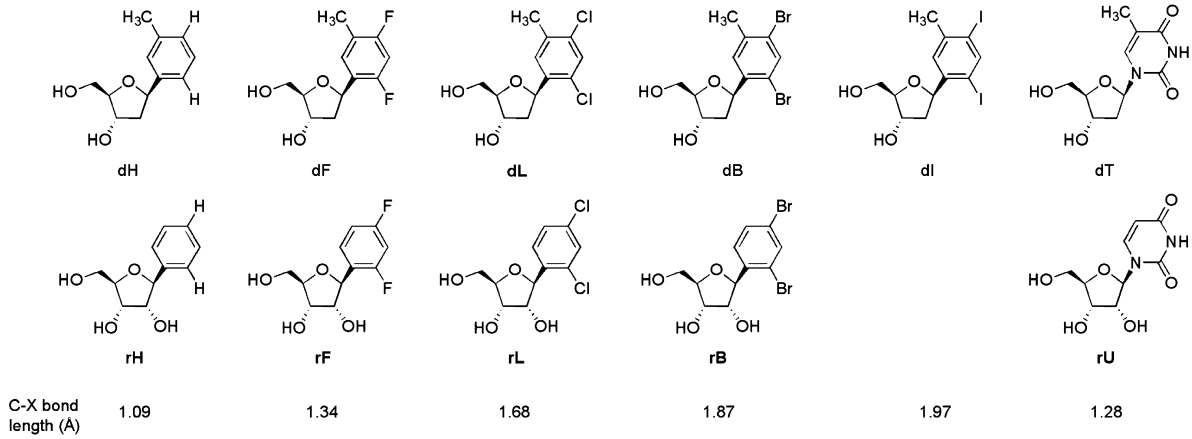

FIGURE 1: Structures of nonpolar thymidine and uridine base analogues with gradually increasing size.

to that of the natural base. Remarkably, changes in size beyond this optimum as small as 0.4 Å led to decreases of 100-fold in activity.

Subsequent kinetics studies with T7 DNA polymerase, a higher-fidelity polymerase, showed an even more highly constrained and rigid active site, with differences across the series of 400-fold in efficiency (*7*). In contrast to this, the low-fidelity polymerase Dpo4, a Y-family repair enzyme, showed only a 30-fold difference, demonstrating a considerably more flexible active site (*15, 16*).

Taken together, these results suggest a strong relationship between active site rigidity and replication efficiency and fidelity in two families of DNA polymerases. However, few studies exist on the steric flexibility of reverse transcriptases, a distinct family of DNA-polymerizing enzymes (*17*). As mentioned above, the fidelity of HIV-RT with RNA templates has been measured to be lower by several-fold than with DNA templates (*5, 6*); thus it would be of interest to explore whether the steric constraints of these two activities differ as well. Gaining a better understanding of the active site constraints in HIV-RT will contribute to our overall knowledge of the origins of mutagenesis involving this low-fidelity enzyme.

To begin to address this issue, we have carried out a study on the active site steric constraints for the DNA-templated polymerization activities of HIV-RT, using steady-state kinetics methods to evaluate activities with thymidine analogues of varied size. Comparison with recent data for the RNA-templated activity (*18*) shows that the DNA-dependent and RNA-dependent polymerase activities have different sensitivities to systematic steric perturbations in the active site, suggesting a possible origin of the lower fidelity when copying RNA sequences.

RESULTS

Variably Sized Thymidine and Uridine Analogues. Structures of the deoxyribonucleoside and ribonucleoside analogues in this study are shown in Figure 1. The DNA thymidine analogue series was synthesized as previously reported (*11*). The RNA uridine analogues containing hydrogen, fluorine, chlorine, and bromine substituents (rH, rF, rL, and rB, respectively) were synthesized as described (*19–22*). A hypothetical diiodo-substituted variant (rI) was not included because of difficulties in synthesis, as recently reported (*18*). Phosphoramidite derivatives of these analogues were used in the synthesis of DNA and RNA templates containing the modified bases; these were characterized previously (*14, 18*). In addition, 5′-triphosphate derivatives of the deoxy series were prepared for enzymatic primer extension reactions (*14*).

Single Nucleotide Incorporation/Extension Reactions and Data Analysis. Steady-state single nucleotide incorporation and single nucleotide extension experiments were performed with a 28-mer/23-mer or 28-mer/24-mer template−primer duplex, respectively (sequences are given in the Experimental Procedures section). For incorporation experiments, the unnatural base was either the incoming dNTP or was positioned in the template to pair with an incoming natural dNTP. We also measured the steady-state kinetics for extension beyond single A•X and T•X base pairs, where X denotes an unnatural base of the series. Radiolabeled products of single nucleotide addition were resolved from unreacted primer by 20% denaturing polyacrylamide gel electrophoresis, and the amounts of incorporation were quantified by autoradiography. By use of varying concentrations of dNTP, we determined V_{max} and K_M values from Hanes−Woolf plots of ([dNTP] vs [dNTP]/v); tables with the data can be found in Supporting Information. Enzymatic efficiency was defined as V_{max}/K_M, and fidelity was defined as the efficiency for the correct base pair (since the unnatural bases are all thymidine or uracil mimics, adenine was considered the correct pair in all cases) divided by the efficiency for the most efficient mismatch.

DNA Polymerase Activity of Wild-type HIV-RT. Data for single nucleotide incorporation kinetics experiments using DNA templates are given in Tables S1 and S2 (Supporting Information), and are compared graphically in Figure 2. Results are given both for the unnatural bases in the DNA template at the site of incorporation with natural dNTPs and unnatural DNA templates (Figure 2A), and with unnatural incoming dNTPs with natural DNA templates (Figure 2B). Adenine was found to be the preferential partner for all the thymidine mimics except for the largest analogue (dI) in the template, for which dTTP was slightly more efficiently incorporated than dATP. In general, the most efficient mismatch opposite the analogue bases was thymine, while pairing with guanine and cytosine was highly inefficient or was not observed at all. Nucleotide incorporation efficiency was usually substantially better when an unnatural base was in the template as compared with it being the incoming

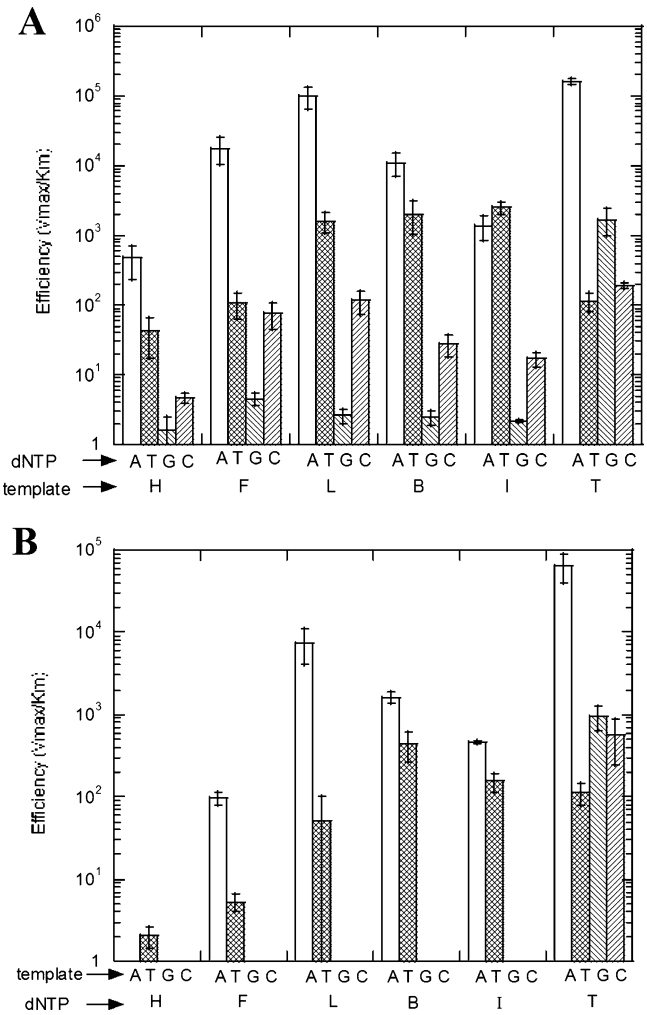

FIGURE 2: Effect of varying base size on steady-state kinetic efficiencies for single nucleotide insertion by HIV-RT. (A) Insertion of natural dNTPs opposite variably sized thymine analogues in the DNA template, with a natural T template shown for comparison. (B) Insertion of analogue deoxynucleoside triphosphates opposite natural DNA template bases, with dTTP shown for comparison. Empty columns indicate that no incorporation was observed under any conditions tried ($V_{max}/K_m < 1$).

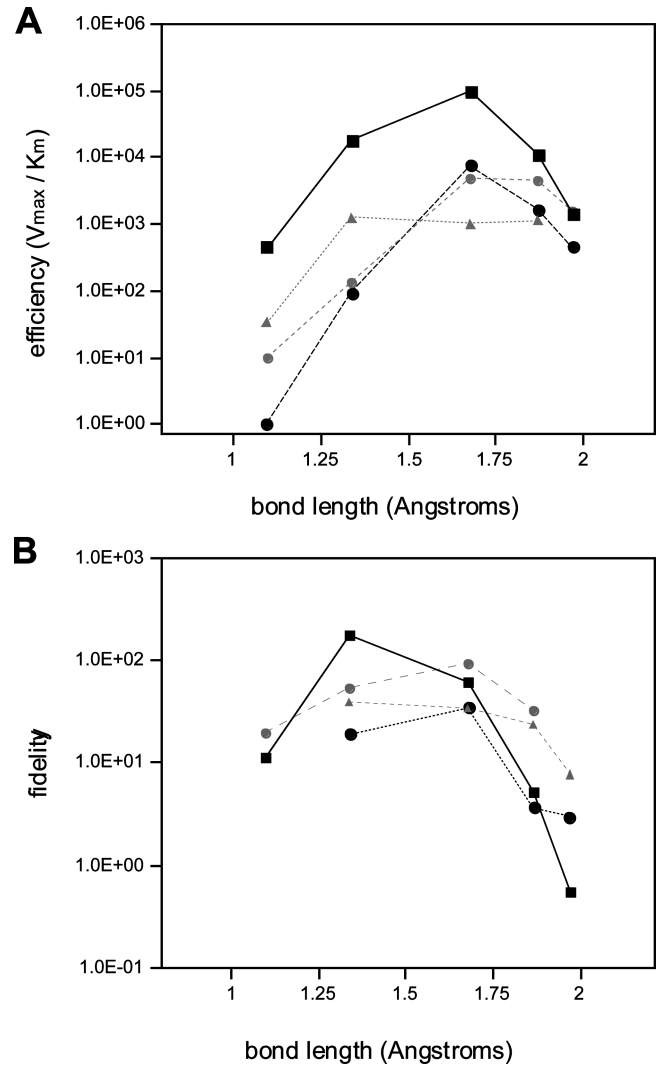

FIGURE 3: Effect of base size variation on nucleotide incorporation efficiency (A) and fidelity (B) of HIV-RT, showing greater size dependence with a DNA template over an RNA template. The *x*-axis shows variable bond length of analogues (see Figure 1). Fidelity is defined as incorporation efficiency with correct partner (adenine) divided by incorporation efficiency of the best mismatched base (thymidine for analogues). (●), Natural DNA template with analogue dNTPs; (■), analogues in DNA template with natural dNTPs; (gray triangle), analogues in RNA template with natural dNTPs (*18*); (gray circle), natural RNA template, analogue dNTPs (*18*).

dNTP, an outcome previously seen for the Klenow fragment of DNA polymerase I (Kf) (*23*).

Incorporation efficiency for A·X base pairs varied by 210-fold (depending on size) when the thymidine mimics were template base analogues, and by 78-fold when they were incoming dNTPs (Tables S1 and S2; plotted in Figure 2). The optimal size for the analogue series occurred with the dichlorotoluene (dL) analogue, which acted as a template with efficiency virtually the same as natural thymine. The same size preference was found in the incoming nucleotide series, with dLTP being only 8.6-fold less efficient than dTTP as an incoming triphosphate derivative (Figure 2B). Efficiency dropped off steeply as size decreased from this maximum, particularly for unnatural dNTPs, with no observable incorporation of dHTP opposite template A. As size increased beyond the optimum, efficiencies of nucleotide incorporation decreased by a maximum 2 orders of magnitude, both for the analogues in the template or as incoming nucleotides (Figures 2A and B). Figure 3A shows a plot comparing the size dependence of base pair synthesis efficiency for DNA versus RNA templates. The plot shows that the efficiency varies considerably more with size with the DNA template, whether the variably sized analogues are in the template or are dNTP analogues.

The fidelity of pairing of the thymine shape analogues with adenine was determined from the ratio of X·A pair efficiencies divided by X·T efficiencies (the most efficient mismatch) and is plotted in Figure 3B. The results show that this fidelity is also related to size (as previously observed for the Kf enzyme) (*14*), with the highest fidelity for analogue dL when the unnatural bases are in the template, and for dFTP when the unnatural bases are incoming nucleoside triphosphates. The fidelities for the thymidine analogues in these respective cases are close to the value we measured for natural thymidine (see Tables S1 and S2, Supporting Information). As size increased beyond the optimum, the fidelity dropped markedly, and the largest unnatural analogue (dI) displayed equally efficient pairing with A or T. We note

that our measured value for fidelity with the natural thymidine template is 9-fold lower than the previously reported steady-state value (*5*). This may be due to the use of a different sequence context than the prior studies.

The incorporation efficiencies and fidelities for RNA templates (from previously published data) (*18*) are shown in comparison to the analogous DNA plot in Figure 3; the DNA plots (Figure 3) show a steeper dependence on size than is seen with the RNA templates. With RNA, the data showed that dLTP, dBTP, and dITP were all incorporated opposite the most efficient mismatch, uracil, with roughly equal efficiency. Fidelity was low for the rH template, but varied only by about 3-fold between rF, rL, and rB, again confirming high flexibility to size increases. Overall, the data plotted in Figure 3 are indicative of greater active site rigidity of HIV-RT when the template is DNA as compared to RNA.

Steric Response to Extension Beyond Variably-Sized Pairs. Steady-state kinetics measurements were next performed to evaluate steric responsiveness of HIV-RT in the extension step. Experiments were carried out with both DNA template and RNA templates (extension was not studied in the previous report (*18*)). We employed templates hybridized to a DNA primer having one additional base (as compared with the above insertion experiments), either adenine or thymine, at the 3′ terminus. This extra base was paired opposite template bases with varied size, and single nucleotide incorporations beyond this variably sized pair were measured. Kinetics data are tabulated in Tables S3 and S4 (Supporting Information), and are shown graphically in Figure 4.

Results for the extension on DNA templates showed that there was a high degree of tolerance for extension beyond large pairs, with extension efficiencies dropping only slightly across the dL/dB/dI series. For pairs smaller than the optimum (dL), extension beyond A·H and A·F base pairs was inefficient, with a loss of 17-fold in efficiency compared with dL. Notably, extension beyond mismatched T·X pairs was nearly as efficient as extension past the matched A·X pair, varying less than 2-fold for all the unnatural analogues. This was also observed for a natural mismatch (T·T), where extension was only about 2.4-fold less efficient than that for a natural A·T pair (*24*). Taken together, the results show that the DNA polymerase activity of HIV-RT is sensitive to size changes in the nucleotide insertion step, but is considerably more flexible in accepting increases in the size of the terminal base pair in the extension step.

The DNA template extension data also show a significant beneficial effect of the polar H-bonding groups, with a 63-fold decrease in efficiency for extension beyond the A-F pair as compared with an A-T pair. This lowered extension efficiency was observed in previous qualitative experiments and was attributed to the lack of a minor groove hydrogen bond between the polymerase and the DNA template strand (*25*).

Next, we studied extension beyond variably sized pairs using RNA templates. Numerical data are in Table S4 (Supporting Information) and are plotted in Figure 4B. Interestingly, results showed that extension on the RNA−DNA duplexes was somewhat more sensitive to base size than that seen for the DNA−DNA duplex (compare Figures 4A and B). Efficiency with suboptimal base sizes was relatively low, and no extension at all was observed past the smallest cases

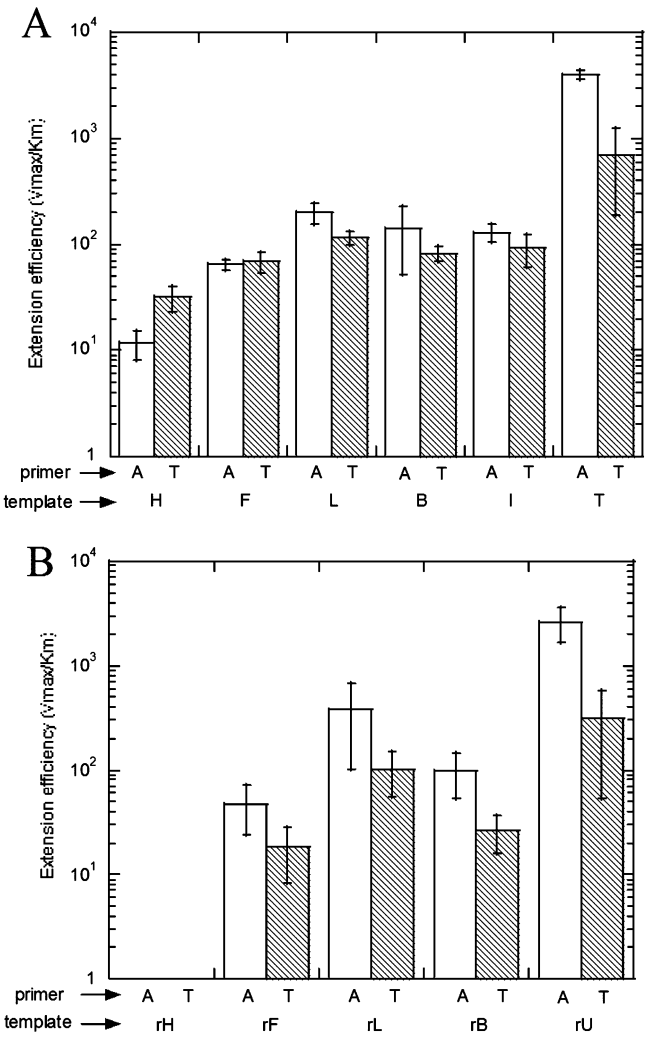

FIGURE 4: Effect of varying base pair size on extension. Shown are steady-state efficiencies for extension beyond A·X and T·X pairs, where X is a nonpolar thymidine or uracil analogue of varying size. (A) Extension efficiencies with DNA templates. (B) Extension efficiencies with RNA templates. Empty columns indicate that no extension was observed under any conditions tried.

(involving the rH analogue). Increasing size beyond the dichloro-substituted optimum showed a greater drop in efficiency on increasing by one step (to rB) than the DNA−DNA case showed for an increase of two steps in size (dL to dI). The most efficient extension was past an A·rL base pair, which was 77-fold less efficient than extension beyond a natural A·rU base pair, similar to the above observation with the dL-containing template. Extension beyond T·X pairs was 2- to 4-fold less efficient than extension past A·X pairs, which is a slightly higher mismatch sensitivity than observed (above) for the DNA−DNA template.

DNA Polymerase Activity of HIV-RT Mutants with Altered Fidelity. To evaluate whether altered-fidelity mutants of HIV-RT display measurably different steric sensitivity as compared with the wild-type enzyme, we carried out single nucleotide incorporations of natural dNTPs opposite the variably sized DNA template base analogues for the F61A (*26*) and K65R (*27*) mutants. Both mutants were reported to exhibit higher fidelity than the wild-type enzyme using genetic assays, although no single nucleotide insertion kinetics studies had previously been carried out. Our kinetics

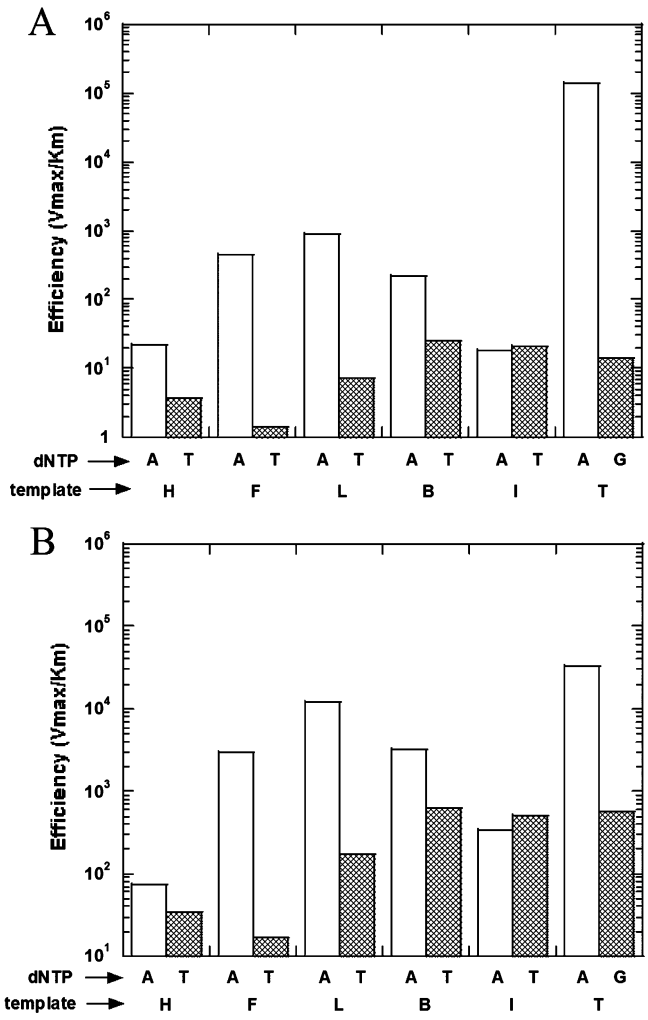

FIGURE 5: Steady-state kinetic efficiencies for single nucleotide incorporations with two HIV-RT mutants. Data are for the incorporation of natural dNTPs opposite DNA template base analogues, with a natural T template shown for comparison. Data for the correct dNTP, dATP, and the best mismatch, dTTP for template base analogues or dGTP for natural T, are shown. (A) F61A mutant. (B) K65R mutant.

data are listed in Table S5 and S6 (Supporting Information) and are graphed in Figure 5. Results of steady-state kinetics studies for the F61 mutant showed that efficiency varied 50-fold across the series (Figure 5A), whereas the wild-type enzyme had a >200-fold range (see above). The overall trend was similar to that of the wild-type enzyme (see Figure 2A), with dATP insertion efficiency peaking with dL in the template and decreasing for larger and smaller analogues. However, dATP was inserted opposite the nonhydrogen-bonding analogue dL 160-fold less efficiently than opposite natural dT; this was substantially different from the wild-type enzyme, for which a template dL was virtually as efficient as natural dT. The fidelity with the analogues (i.e., the ratio of dATP efficiency to dTTP efficiency) peaked at dF (1.2×10^2) and was lowest for dI, which showed a slight preference for a T•T mismatch. Significantly, the fidelity of F61A for the insertion of natural nucleotides was 10^4, which is 100-fold higher than the value we obtained for the wild-type enzyme with this template sequence.

For the K65R mutant, the efficiency of dATP insertion opposite the analogues varied 160-fold across the series, showing a greater range than the F61A mutant (Figure 5B) but slightly less than the wild-type enzyme. A significant difference, however, was that dATP was incorporated opposite the best analogue, dL, only 30-fold less efficiently than opposite natural dT. Efficiency for dATP incorporation dropped by 35-fold as size was increased from the dL to dB and dI analogues, a similar decrease as seen for the F61A mutant. The fidelity of dATP insertion was greatest for a template dF (1.7×10^2, very close to that of F61A) and decreased as size increased from there. The fidelity of K65R with natural nucleotides being inserted opposite a template dT was 6.1×10^2, about 6-fold higher than what we measured for the wild-type enzyme in this context.

Comparisons of steric responses of the three enzymes (the two mutants and wild-type HIV-RT) with DNA templates can be made from the plots in Figures 5 and 2A. In general, the response to varied base pair size was quite similar for the three, with the same size optimum (the dichlorotoluene−adenine pair). The chief differences were (1) that the two mutants displayed slightly less kinetic penalty for larger and smaller sizes than did the wild-type enzyme and (2) that the F61A mutant showed substantially lower activity in the absence of hydrogen bonding than did the WT or K65R enzymes.

DISCUSSION

Our data demonstrate that the DNA template-dependent DNA polymerization (DDDP) and RNA-dependent DNA polymerization (RDDP) catalytic functions of HIV-1 RT differ by a surprising degree in their functional steric sensitivity. For nucleotide insertion, the DNA-dependent activity decreases in efficiency by approximately 20–70-fold on increasing the size of a thymidine analogue by 0.3–0.5 Å from the optimum. By contrast, the RNA-dependent (RDDP) efficiency drops by only 0–3-fold (Figure 3A), which is remarkable, given that the same enzyme active site is involved. The relatively lower steric sensitivity of the RDDP activity is consistent with earlier reports that the activity with an RNA template operates with lower fidelity than with a DNA template (*5, 6*). Since one important mechanism by which polymerases may enforce correctness of base pairing during nucleotide selection is by rigid enforcement of canonical pair size and shape (*7, 14, 28*), the greater flexibility with an RNA template may lead to the acceptance of mismatched (and thus sterically altered) pairs at lower energetic cost.

What is the origin of this apparent difference in steric selectivity and of the presumably related difference in fidelity? This difference must reflect the inherent structural or dynamic difference between DNA−DNA and DNA−RNA duplexes and their interactions with the surrounding active site. An X-ray crystal structure of this enzyme complexed with a DNA−DNA duplex shows that the DNA adopts an A-like structure (*29*). Although no RNA−DNA duplex costructure is yet available for comparison, the RNA−DNA structure is also likely to be A-like since that is the inherent preference for RNA−DNA heteroduplexes. Thus, no large conformational difference that might affect active site interactions seems likely, although it cannot be ruled out without more structural studies of the RNA−DNA complex with HIV-RT.

We hypothesize that one possible origin for the difference in fidelity between the DNA-templated and RNA-templated

activities in this enzyme may be the lack of a C-5 methyl group in uracil as compared with thymine. We note that our primer−template sequence contains A-T(U) in two of the last three terminal positions. A methyl group in the template major groove (with a template T) is expected to make contact with the enzyme, whereas a missing methyl (as with U) would leave space and therefore room for larger (or mismatched) base pairs. Reverse transcriptases in general must leave sufficient space for this methyl group (or sufficient flexibility to adapt to it) since they retain DNA-templated activity along with RNA-templated activity. This leads to a number of testable predictions. For example, replication of runs of DNA that lack T should be processed with the same lower fidelity that the analogous RNA would be. In addition, removal of methyl groups in DNA templates should result in lower fidelity, while the addition of methyl groups to synthetic RNA templates should increase fidelity. Future experiments will address these possibilities.

Aside from this hypothesized methyl effect, we considered other possible contributing factors to the lower fidelity with RNA templates. For example, a different conformation for the RNA−DNA helix in the active site might lead to different side chain contacts and to different enzyme conformational adjustments in response to base pair sizes. However (as mentioned above), this seems unlikely because of the A-like structure of the DNA helix in the active site. One may also consider the possibility that localized side chain interactions with the 2′-hydroxyls of RNA template residues might in some way affect enzyme motions. Molecular dynamics simulations may be useful in evaluating this possibility once more becomes known about the structure of the RNA−DNA−nucleotide ternary complex with HIV-RT.

A comparison to previous data shows that the DDDP activity of HIV-RT is similarly constrained (in the steric sense) to that of the Klenow fragment of DNA Pol I (Kf exo-) (*14*). Like Kf exo-, efficiency differences of over 2 orders of magnitude are observed for HIV-RT when the size of the incoming dNTP or the templating base are varied by less than 0.5 Å from the optimally sized thymidine analogue. The optimum for incorporation or extension with HIV-RT (both DDDP and RDDP) is the dichloro case (dL, rL), which forms a base pair with adenine that is ~0.5 Å larger than a T·A pair. The same preference for a larger-than-natural base is also seen for Kf exo- (*14, 30*). Thus, both Kf exo and HIV-RT (DNA pol function) fall into an intermediate range of fidelity and steric sensitivity; T7 DNA polymerase is a higher-fidelity enzyme that is both more rigid and tighter in its steric responses than Kf (*7*), while the low fidelity Dpo4 enzyme is much more insensitive to steric size changes (*15*).

Also consistent with our results are findings of Marx, who investigated the DNA-templated polymerase activity of HIV-RT with nucleotide analogues having substituents on deoxyribose, at the C-4′ position, thus increasing their steric size. Kinetics experiments with the wild-type enzyme showed that HIV-RT was sensitive to increased sugar size, but that a mutant (M184V) allowed more steric room and was complemented by sugars having increased size (*17*). Similar data for the RNA-templated activity are not yet available.

The HIV reverse transcriptase is an error-prone enzyme, and much of its low fidelity arises from its poor discrimination against extension of mismatches (*5, 31*). Indeed, with the natural nucleotides, we observed quite low fidelity for extension (only a 6-fold kinetic discrimination against a mismatch). Our data from probing the steric sensitivity of base pair extension is consistent with the notion that the active site is quite sterically flexible in accommodating variably sized bases. This is especially the case for the DNA template, where increasing a thymidine analogue's size from the optimum (dL) to the maximum (dI) resulted in only a 1.5-fold decrease in activity. Also consistent with this is the fact that extension beyond sterically mismatched T-analogue pairs is nearly as efficient as extension past A-analogue pairs. Interestingly, the base pair extension efficiencies of DNA-templated and RNA-templated DNA synthesis activities also differ somewhat in their steric responses, but in the opposite way. For extension, the RDDP activity drops off in efficiency by as much as 200-fold for suboptimal size, whereas with the DDDP extension, it drops by 17-fold at most. The reasons for this difference are not yet clear.

In addition to testing the steric response of this enzyme, our data provide insights into the hydrogen-bonding requirements of HIV-RT. The current experiments suggest that the wild-type HIV-RT enzyme shows relatively little sensitivity to a loss of hydrogen-bonding potential in the incipient base pair. Direct comparison of the activity with thymine and its isosteric analogue difluorotoluene show, for example, that dF in a template is only 9-fold less efficient than dT, and the optimally sized compound (dL) is only slightly less efficient than the natural compound. This small loss of activity is similar to that seen for Kf enzyme (*14, 32*), suggesting a similarly small benefit from Watson–Crick hydrogen bonding in the HIV enzyme. Importantly, the fidelity against mismatch formation by the DNA polymerase function of HIV-RT is virtually the same regardless of whether natural or non-H-bonding thymine analogues are involved. This is also true for the RNA-templated activity, where rF is processed with fidelity similar to that of natural rU. This again points to steric rather than electrostatic effects as being dominant in determining the fidelity of nucleotide insertion for this enzyme.

However, a hydrogen-bonding contribution in the ultimate pair for base pair extension (in both DNA- and RNA-templated modes) appears to be more substantial since the optimal nonpolar analogues in extension (dL or rL) remain significantly below natural pairs in their efficiency. An early survey of several polymerases with analogue dF suggested that the main factor for HIV-RT in low extension efficiency is a lack of minor groove hydrogen-bonding ability (*25*). Examination of a published X-ray crystal structure (*29*) suggests that side chains Y115 and/or Y183 make hydrogen-bonded contacts in the minor groove of the template strand, and our kinetics studies suggest that loss of such a contact (or the cost of desolvation of the side chain) contributes a significant loss of efficiency at the transition state for base pair extension.

It is well known that mutations of HIV-RT can alter its fidelity, and it has been suggested that changes in active site flexibility may be responsible (*33*). The current experiments represent the first systematic probing of this flexibility for two such mutants. Our data with the F61A and K65R enzymes represent the first full kinetics measurements for these two polymerases, and show that fidelity is increased by a factor of 6 for K65R and by a factor of 100 for F61A. This confirms previous reports that the mutants both have

increased fidelity for nucleotide incorporation relative to wild-type HIV-RT (*26, 27*). Interestingly, both show little change in kinetic sensitivity (vs wild-type) to the base size variations tested here, but both show an apparent increase in dependence on hydrogen-bonding groups. For example, the higher-fidelity mutant (F61A) is 160-fold less active at nucleotide incorporation opposite a nonpolar analogue (dL) than opposite thymine, whereas the wild-type enzyme is only 1.6-fold less active. The low steric sensitivity of the K65R mutant may not be surprising, given that the Lys-65 residue makes contacts with the γ-phosphate residue of the incoming nucleotide but not with the base pair (*29*). The Phe-61 residue also does not contact the incipient pair but does contact the template strand near this pair.

While the physical origin of this increased H-bonding dependence is not clear, it is possible that this difference is related to the substantially higher fidelity of this enzyme. We recently observed a strong H-bond dependence in a high-fidelity β3-β4 loop deletion mutant and in the K65R mutant (*34*). However, we have also observed strong hydrogen-bonding dependence in a low fidelity Y-family enzyme (Dpo4) (*15*). Taken together with previous results, the current findings suggest that there are multiple mechanisms by which fidelity can be affected by physical properties of polymerases. Previous studies of three natural enzymes (Kf exo-, T7 DNA polymerase, and Dpo4 polymerase) have observed a relationship between steric sensitivity (enzyme flexibility) and fidelity (*7, 14, 15*). The current findings with mutants of a different polymerase family show that it is also possible to have increased fidelity without increasing apparent steric sensitivity, at least in the dimension probed here. Our analogue series alters base pair lengths, which is one dimension that may affect fidelity (*8*); however, dimensional changes in shape and size toward the major or minor grooves, or flexibility of the grip on the incoming template strand might also affect the active site tightness. Differently shaped analogues than the present ones may be needed to probe this possibility.

EXPERIMENTAL PROCEDURES

Steady-State Single Nucleotide Insertion and Extension Kinetics. A 28-mer/23-mer template/primer duplex having the sequence 5′-d(ACTGXTCTCCCTATAGTGAGTCGTATTA))•(5′-TAATACGACTCACTATAGGGAGA) or 5′-(r(ACUGXUCUCCCUAUAGUGAGUCGUAUUA))•(5′-d(TAATACGACTCACTATAGGGAGA)) was used as polymerase substrate for insertion kinetics. 24-mer primers extension primer A 5′-d(TAATACGACTCACTATAGGGAGAA) and extension primer T 5′-d(TAATACGACTCACTATAGGGAGAT) were used for extension kinetics. Primers were labeled using [γ-^{32}P]ATP (Amersham Bioscience) and T4 polynucleotide kinase (Invitrogen). Labeled primers were purified using spin columns (Biorad). Primer-templates were annealed by making a 1:1 mixture of primer and template (4 μM each) in Buffer A (200 mM Tris-HCl (pH 7.9) containing 20 mM $MgCl_2$ and 20 mM DTT), then heating to 95 °C, and slowly cooling to 4 °C over 90 min.

Wild-type HIV-RT was obtained from Worthington Biochemicals, and HIV-RT mutants F61A and K65R were prepared as described (*26, 34*). Annealed primer−template was mixed with enzyme (1:1) to make a 2× primer/template/enzyme solution. Kinetics were measured at 37 °C. Primer/template/enzyme solution in Buffer A was mixed with 2× dNTP solution in Buffer B (200 mM Tris-HCl buffer (pH 8.0), 20 mM $MgCl_2$, and 12 mM β-mercaptoethanol), and the reaction was quenched by the addition of stop buffer (95% formamide containing 10 mM EDTA, 0.05% xylene cyanol and 0.05% bromophenol blue). Products were resolved from unreacted primer by 20% denaturing polyacrylamide gel electrophoresis and quantified by autoradiography using a phosphorimager (Molecular Dynamics).

Band intensities on the imaged gels were measured with ImageQuant software (Molecular Dynamics). Reaction velocity v for individual reactions was calculated by the equation $v = I_{n+1}/(I_n + I_{n+1})/t$, where I_n is the intensity of the unreacted primer band, and I_{n+1} is the intensity of the product band for reactions where less than 20% product was formed. Velocities were normalized for enzyme concentration, and V_{max} and K_M values were determined from Hanes−Woolf plots. Efficiency was defined as V_{max}/K_M, and fidelity was defined as efficiency for the correct base divided by efficiency for the most efficient mismatch.

Synthesis of Variably Sized Thymidine Analogues. The synthesis and DNA incorporation of the thymidine analogue series was performed as previously described (*11*). Unnatural dNTPs were prepared as reported (*14*). Ribonucleoside analogues were prepared as described (*18*). Unnatural nucleosides were incorporated into DNA or RNA templates as reported previously (*14, 18*).

SUPPORTING INFORMATION AVAILABLE

Tables of steady-state kinetics data (Tables S1–S6). This material is available free of charge via the Internet at http://pubs.acs.org.

REFERENCES

1. Bebenek, K., Abbotts, J., Roberts, J. D., Wilson, S. H., and Kunkel, T. A. (1989) The fidelity of DNA synthesis catalyzed by derivatives of Escherichia coli DNA polymerase I. *J. Biol. Chem. 264*, 16948–16956.
2. Rausch, J. W., and Le Grice, S. F. (2007) Exploiting structurally diverse nucleoside analogs as probes of reverse transcription complexes. *Curr. HIV Res. 5*, 11–22.
3. Geretti, A. M. (2006) Clinical implications of HIV drug resistance to nucleoside and nucleotide reverse transcriptase inhibitors. *AIDS Rev. 8*, 210–220.
4. Gotte, M. (2006) Effects of nucleotides and nucleotide analogue inhibitors of HIV-1 reverse transcriptase in a ratchet model of polymerase translocation. *Curr. Pharm. Des. 12*, 1867–1877.
5. Yu, H., and Goodman, M. F. (1992) Comparison of HIV-1 and Avian Myeloblastosis Virus reverse transcripase fidelity on RNA and DNA templates. *J. Biol. Chem. 267*, 10888–10896.
6. Hubner, A., Kruhoffer, M., Grosse, F., and Krauss, G. (1992) Fidelity of Human Immunodeficiency-Virus Type-1 reverse-transcriptase in copying natural RNA. *J. Mol. Biol. 223*, 595–600.
7. Kim, T. W., Brieba, L. G., Ellenberger, T., and Kool, E. T. (2006) Functional evidence for a small and rigid active site in a high fidelity DNA polymerase. *J. Biol. Chem. 281*, 2289–2295.
8. Kool, E. T. (2002) Active site tightness and substrate fit in DNA replication. *Annu. Rev. Biochem. 71*, 191–219.
9. Kunkel, T. A., and Bebenek, K. (2000) DNA replication fidelity. *Annu. Rev. Biochem. 69*, 497–529.
10. Echols, H., and Goodman, M. F. (1991) Fidelity mechanisms in DNA replication. *Annu. Rev. Biochem. 60*, 477–511.
11. Kim, T. W., and Kool, E. T. (2004) A set of nonpolar thymidine nucleoside analogues with gradually increasing size. *Org. Lett. 6*, 3949–3952.
12. Guckian, K. M., and Kool, E. T. (1997) Highly precise shape mimicry by a difluorotoluene deoxynucleoside, a replication-

competent substitute for natural thymidine. *Angew. Chem., Int. Ed. 36*, 2825–2828.
13. Kool, E. T., and Sintim, H. O. (2006) The difluorotoluene debate - a decade later. *Chem. Commun. 35*, 3665–3675.
14. Kim, T. W., Delaney, J. C., Essigmann, J. M., and Kool, E. T. (2005) Probing the active site tightness of DNA polymerase in subangstrom increments. *Proc. Natl. Acad. Sci. U.S.A. 102*, 15803–15808.
15. Mizukami, S., Kim, T. W., Helquist, S. A., and Kool, E. T. (2006) Varying DNA base-pair size in subangstrom increments: evidence for a loose, not large, active site in low-fidelity Dpo4 polymerase. *Biochemistry. 45*, 2772–2778.
16. Ling, H., Boudsocq, F., Woodgate, R., and Yang, W. (2001) Crystal structure of a Y-family DNA polymerase in action: A mechanism for error-prone and lesion-bypass replication. *Cell 107*, 91–102.
17. Strerath, M., Cramer, J., Restle, T., and Marx, A. (2002) Implications of active site constraints on varied DNA polymerase selectivity. *J. Am. Chem. Soc. 124*, 11230–11231.
18. Silverman, A. P., and Kool, E. T. (2007) RNA probes of steric effects in active sites: High flexibility of HIV-1 reverse transcriptase. *J. Am. Chem. Soc. 129*, 10626–10627.
19. Peracchi, A., Matulic-Adamic, J., Wang, S., Beigelman, L., and Herschlag, D. (1998) Structure-function relationships in the hammerhead ribozyme probed by base rescue. *RNA 4*, 1332–1346.
20. Guckian, K. M. (1999) Ph.D. Thesis, University of Rochester.
21. Parsch, J., and Engels, J. W. (2002) C-F - H-C hydrogen bonds in ribonucleic acids. *J. Am. Chem. Soc. 124*, 5664–5665.
22. Somoza, A., Chelliserrykattil, J., and Kool, E. T. (2006) The roles of hydrogen bonding and sterics in RNA interference. *Angew. Chem., Int. Ed. 45*, 4994–4997.
23. Moran, S., Ren, R. X., and Kool, E. T. (1997) A thymidine triphosphate shape analog lacking Watson-Crick pairing ability is replicated with high sequence selectivity. *Proc. Natl. Acad. Sci. U.S.A. 94*, 10506–10511.
24. Pandey, V. N., Kaushik, N., Rege, N., Sarafianos, S. G., Yadav, P. N., and Modak, M. J. (1996) Role of methionine 184 of human immunodeficiency virus type-1 reverse transcriptase in the polymerase function and fidelity of DNA synthesis. *Biochemistry. 35*, 2168–2179.
25. Morales, J. C., and Kool, E. T. (2000) Functional hydrogen-bonding map of the minor groove binding tracks of six DNA polymerases. *Biochemistry. 39*, 12979–12988.
26. Fisher, T. S., and Prasad, V. R. (2002) Substitutions of Phe61 located in the vicinity of the template 5′-overhang influence polymerase fidelity and nucleoside analog sensitivity of HIV-1 reverse transcriptase. *J. Biol. Chem. 277*, 22345–22352.
27. Shah, F. S., Curr, K., Hamburgh, M. E., Parniak, M., Mitsuya, H., Arnez, J. G., and Prasad, V. R. (2000) Differential influence of nucleoside analog resistance mutations K65R and L74V on the overall mutation rate and error specificity of HIV-1 reverse transcriptase. *J. Biol. Chem. 275*, 27037–27044.
28. Kool, E. T. (1998) Replication of non-hydrogen bonded bases by DNA polymerases: A mechanism for steric matching. *Biopolymers (Nucl. Acid Sci.). 48*, 3–17.
29. Huang, H. F., Chopra, R., Verdine, G. L., and Harrison, S. C. (1998) Structure of a covalently trapped catalytic complex of HIV-1 reverse transcriptase: implications for drug resistance. *Science 282*, 5787–5792.
30. Sintim, H. O., and Kool, E. T. (2006) Remarkable sensitivity to DNA base shape in the DNA polymerase active site. *J. Am. Chem. Soc. 128*, 396–397.
31. Perrino, F. W., Preston, B. D., Sandell, L. L., and Loeb, L. A. (1989) Extesion of mismatched 3′ termini of DNA is a major determinant of the infidelity of human immunodeficiency virus type 1 reverse transcriptase. *Proc. Natl. Acad. Sci. U.S.A. 86*, 8343–8347.
32. Moran, S., Ren, R. X.-F., Rumney, S., and Kool, E. T. (1997) Difluorotoluene, a nonpolar isostere for thymidine, codes specifically and efficiently for adenine in DNA replication. *J. Am. Chem. Soc. 119*, 2056–2057.
33. Harris, D., Kaushik, N., Pandey, P. K., Yadav, P. N., and Pandey, V. N. (1998) Functional analysis of amino acid residues constituting the dNTP binding pocket of HIV-1 reverse transcriptase. *J. Biol. Chem. 273*, 33624–33634.
34. Garforth, S. J., Kim, T. W., Parniak, M. A., Kool, E. T., and Prasad, V. R. (2007) Site-directed mutagenesis in the fingers subdomain of HIV-1 reverse transcriptase reveals a specific role for the β3–β4 hairpin loop in dNTP selection. *J. Mol. Biol. 365*, 38–49.

BI702427Y